# 論文 / 著書情報
# Article / Book Information

| | |
|---|---|
| Title | EUV diagnostics of pulsed plasma systems |
| Author | S.R.Mohanty, E.Hotta |
| Citation | Journal of Physics: Conference Series, Vol. 208, 012138, pp. 1-8 |
| Pub. date | 2010, 3 |
| DOI | http://dx.doi.org/10.1088/1742-6596/208/1/012138 |
| Creative Commons | See next page |

# License

# EUV diagnostics of pulsed plasma systems



2010 J. Phys.: Conf. Ser. 208 012138

(http://iopscience.iop.org/1742-6596/208/1/012138)

Journal of Physics: Conference Series **208** (2010) 012138 doi:10.1088/1742-6596/208/1/012138

# EUV diagnostics of pulsed plasma systems

**S R Mohanty[1, 3] and E Hotta[2]**
[1]Centre of Plasma Physics, Sonapur, Kamrup-782402, Assam, India
[2] Department of Energy Sciences, Tokyo Institute of Technology, Yokohama 226-8502, Japan

E-mail: smrutirm@yahoo.com

**Abstract.** Extreme ultraviolet (EUV) diagnostics have been a subject of continuing interest for last several decades in the field of space and plasma sciences. In recent days, EUV diagnostics are being widely employed in the laboratories and industries to characterize EUV emission from the EM radiation sources that have strong impacts on future technology. This paper gives description of some of the important EUV diagnostics such as EUV photon detector, EUV energy measurement system, EUV pinhole camera, grazing incidence spectrograph and transmission grating spectrograph employed at Tokyo Institute of Technology to characterize EUV emission from the low current (<15 kA) and low energy (~ ten of Joule) pulsed plasma systems and some typical results.

## 1. Introduction

Extreme ultraviolet (EUV) diagnostics have been a subject of continuing interest for the last several decades in the field of space and plasma sciences [1-5]. EUV has proved to be a valuable wavelength for the study of particular groups of astronomical objects, including white dwarf stars and stellar coronae, as well as the interstellar medium. Using EUV telescope, the probing of interstellar space and extended atmospheres around stars becomes now a routine work. Moreover, the proper study of extragalactic objects would not be possible without the development of diagnostics at EUV wavelength [1]. Similarly, in the past, tokamak researchers had attempted to study the transport and other physical properties of plasma using EUV and soft X-ray lines emitted by highly ionized plasmas [2]. A renewed interest on EUV spectra measurements from tokamak and other plasma systems are noticed because of the need of generation of atomic physics data in support of the future large fusion devices [4, 5]. The prospect of the employment of EUV and soft X-ray sources for next generation lithography system ($\lambda$ = 13.5 nm), microscopy in the "water window" ($\lambda$ = 2.3 nm – 4.4 nm), plasma diagnostics and EUV/soft X-ray laser research have led to considerable progress on the development of high spatial and temporal EUV diagnostics in recent years [6,7]. The extreme ultraviolet (EUV) plasma sources will become the next generation lithographic source only when the significant obstacles such as in-band EUV energy, small EUV emission volume, spectral purity, positional and energy stability are to be addressed [8-11]. Although the final goal is to produce a suitable 13.5 nm light source, solving the full range of issues and this requires a more thorough understanding of the plasma that emits the EUV optical emissions. Because of the complex nature and extreme conditions produced in the EUV plasma sources, several plasma diagnostics are needed to fully characterize these extreme ultraviolet lithography (EUVL) sources.

 

This paper describes the development and employment of some EUV diagnostics at Tokyo Institute of Technology for characterizing the EUV emission from the pulsed plasma systems namely, capillary [12,13] and gas jet Z-pinch [14,15]. The performance of these EUV emitting sources have been investigated in terms of various technological aspects of EUV lithography. Some important results are presented over here.

## 2. Methodology

The spectral as well as electrical performance of our EUV systems have been evaluated by employing diagnostics such as EUV photon detector, EUV mini calorimeter (energy measurement system), EUV pinhole camera, EUV spectrographs and some routine diagnostics like voltage and current probe etc. Since the motivation behind this work is how to achieve high flux of EUV photon at 13.5 nm, therefore, EUV diagnostics were developed that mainly scanned the wavelength range of 5 to 20 nm. The time evolution of EUV photon in the wavelength range of 5 to 18 nm was monitored using an EUV photodiode (IRD, AXUV-10) coupled with Zr/C filter (thickness 200/50 nm). The choice of photodiode basically depends upon the quantum efficiency of the semiconductor materials in the desired wavelength and the capacitance of the diode. Besides an EUV mini calorimeter, comprising of a Zr filter, Mo/Si multi-layer mirror and photodiode was used for the absolute in-band power measurement. The Zr filter used in this detector is transparent to the wavelength range of approximately 12 to 18 nm. The multilayer mirror is coated with 50 bilayers of Mo/Si having maximum reflection at 13.5 nm and the bandwidth of the stack is typically 0.5 nm. Since the reflectivity of multilayer mirror is maximum at 45° incident angle, the mirror was positioned accordingly with respect to the incoming EUV light. The calorimeter was calibrated by JENOPTIK energy monitor [12]. The EUV pinhole camera consisting of a 50 μm diameter pinhole, a Zr filter and an X-ray CCD camera (Andor Technology Ltd. DO434) was used for measuring the dimension of the EUV emitting volume and for evaluating the positional stability of the EUV emitting zone. The resolution of the pinhole camera which is limited by the diameter of the pinhole and by the diffraction is found to be around 100 μm. For recording the wavelength of EUV emission, a grazing incidence spectrograph and transmission grating spectrograph were employed. Commercially available McPherson flat-field grating spectrometer (model 248/310G) was used for the investigation of photon emission in 10 to 20 nm wavelength range. It mainly consists of an entrance slit, a 600 grooves/mm diffraction grating and a microchannel plate (MCP) intensifier. The resolution of the spectrometer is of the order of 0.036 nm. In addition to the grazing incidence spectrograph, a transmission grating spectrograph was designed in house and employed for recording the photon emission mainly in 3 to 50 nm wavelength range. A transmission grating of 1000 lines/mm in normal incidence geometry, a 50 μm pinhole and an X-ray CDD camera were basically used to fabricate the transmission grating spectrometer. A spectral resolution of 0.45 nm is obtained by optimizing the aperture, the source to grating distance and the grating to detector distance. For the routine check of electrical signal at the different parts of the circuit, commercially available voltage and current probes were used.

The pulsed plasma systems used in the present work, based on the well-known principle “pinch effect”, generate a high-temperature and high-density transient plasma that emits copious amount of EUV radiation in the expense of electrical power. Two compact pulse power drivers were designed and constructed that pump the electrical power into the pulsed plasma systems. These comprise of a high voltage power supply, pulse forming network, spark gap switch, pulse transformer, magnetic switch, capacitor bank etc. The details of the pulse power drivers are described elsewhere [12]. One pulse power diver, named as the slow pulse power driver, delivers a low dI/dt of around 20 A/ns at the load. On the other hand, the other pulse power driver, named as fast pulse power driver, produces a high dI/dt of the order of 57 A/ns at the discharge part. The brief outlines of the different discharge heads employed in the present work are described hereafter.

The capillary discharge head comprises of mainly a narrow ceramic tube sandwiched in between specially configured coaxial electrodes as shown in figure 1 (a). A 10 mm long alumina capillary having inner diameter 2 mm is rigidly fixed in between two molybdenum electrodes. The electrode

structures are specially designed so as to reduce the surface current density, to have a laminar flow of Xenon (Xe) gas and to collect adequate EUV light flux. Besides the electrode design features accommodate the water-cooling arrangement and thus enables to have a low rate of electrode material erosion.

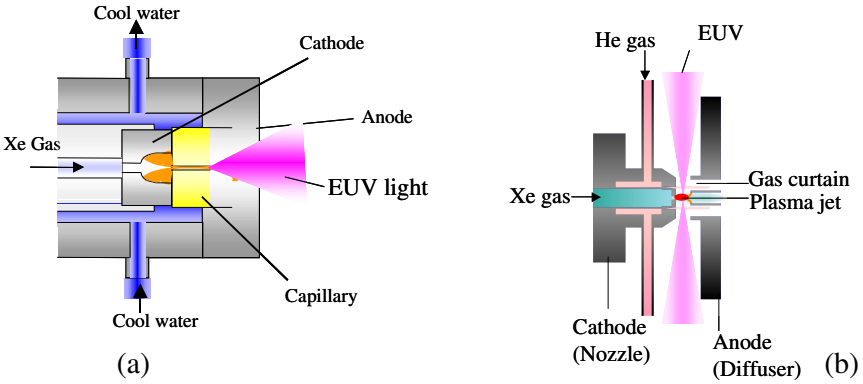


**Figure 1.** Different pulsed plasma discharge heads, (a) capillary and (b) gas jet z-pinch

The gas jet Z-pinch discharge head has the uniqueness of a jet type coaxial electrodes configuration as shown in figure 1 (b). The electrodes configuration of this source has typically a dual orifice nozzle (cathode) and corresponding diffuser (anode). The dual orifice nozzle consists of two simplex nozzles arranged concentrically. The inner nozzle have 2 mm mouth diameter and the outer nozzle having annular cylindrical type opening have 1 mm width. The annular separation between the inner and outer nozzle is 4 mm. The inner and outer diameters of the diffuser are 6 and 24 mm, respectively. The inner nozzle supplies the source gas (xenon) for the EUV light and the outer nozzle supplies helium gas for the gas curtain. The typical design parameters of the nozzles and pressure inside the detection chamber help to maintain a subsonic gas flow through the nozzles.

The discharge head is mounted inside the detection chamber through one of its port as illustrated in figure 2. The detection chamber has another five ports that are used for diagnostic purposes as well as evacuation. The detection chamber is usually evacuated up to a base pressure of less than mTorr with the aide of a turbo pump. Xe gas is fed into the discharge head with the help of mass flow controller. The supply gas pressure and chamber pressure are monitored using Baratron pressure transducer. The pressure of the xenon gas near the discharge head is to be controlled up to several hundreds mTorr while the chamber pressure is maintained less than several mTorr.

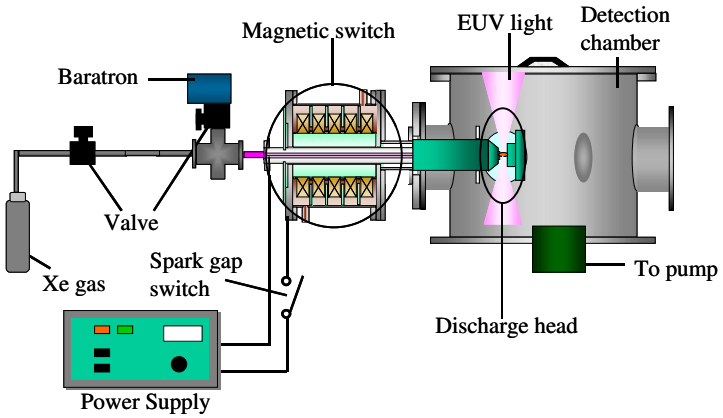


**Figure 2.** Schematic of the EUV experimental setup

## 3. Results and discussion:

Numerous experiments were conducted in each discharge head to find out the discharge dynamics and the optimum EUV emission by varying different experimental conditions. Both the pulse power drivers were at first employed to check the performance of capillary discharge head and it was found that the fast pulse power driver with high dI/dt emits more stable and intense EUV emission. The significant findings on each discharge head driven by the fast pulse power supply are mainly discussed in this paper.

The electrical measurements indicated that our fast pulse power driver delivered around 10 kA discharge current and 25 kV discharge voltage across the capillary head to create hot and dense plasma, which emits photons mainly in the EUV region.

The time evolution of EUV emission was compared with the discharge current pulses for various experimental conditions using EUV photodiode. A typical set of traces of the discharge current and photodiode signals recorded at 5 Torr supply pressure and 9 kV charging voltage is shown in figure 3. The traces indicate that the EUV photons emerge out after 40 ns of the initiation of discharge inside the capillary and the photon emission reaches a peak value during the maximum of discharge current. The pressure inside the capillary was varied from 2 to 8 Torr in order to find out the optimum pressure condition for the maximum EUV output. It is observed that the EUV emission is maximum at a pressure of around 5 Torr.

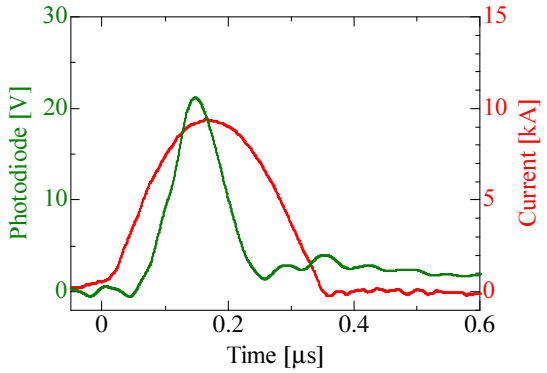


**Figure 3.** Traces of EUV output and current signals

The EUV mini calorimeter was used to evaluate the absolute in band radiation at best operating conditions. It is estimated be maximum of 3.3 mJ/sr/2%BW/pulse at optimum operating condition [12]. The angular variation of EUV measurement shows that EUV emission is fairly symmetrical except at 10° angle as illustrated in figure 4.

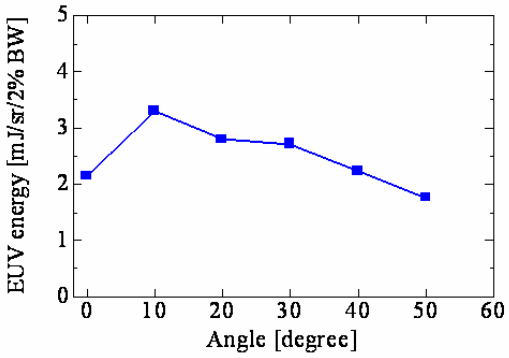


**Figure 4.** Angular distribution of in-band radiation

The EUV pinhole camera was employed on axis (0°) and off axis (45°) of the capillary plasma system to record the images of EUV emitting zone in various experimental conditions like different supply pressures and charging voltages. Figure 5 shows a typical on axis and off axis EUV images obtained for the best operating condition (9 kV charging voltage and 5 Torr supply pressure). The images obtained on axis and off axis are circular and ellipsoidal in nature, respectively. The images recorded on axis seem to be fairly symmetric with respect to the capillary axis irrespective of the gas pressure. The high intensity zone is reasonably symmetric to the total EUV emitting zone. With the increase in supply gas pressure, the EUV emission region seems to be ejected out of the capillary. The size and intensity of EUV plasma strongly depend upon the gas pressure. The source dimension having length of 0.143 mm and diameter of 1.103 mm is estimated form the pinhole images at optimum condition. The positional and pulse-to-pulse intensity stability were also evaluated from pinhole imaging and quite encouraging results are obtained.

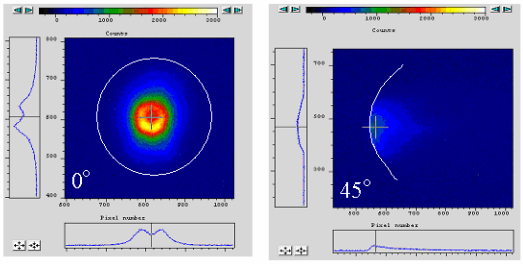


**Figure 5.** Typical on axis and off axis pinhole images

The time-resolved EUV emission spectrum from the capillary discharge head was carried out using the McPershon spectrometer. The slow power supply was used to power the discharge head and observation was carried out on entire time range corresponding to the slow current pulse. Two typical time-gated spectra recorded after 450 and 700 ns of the initiation of discharge are shown in figure 6. The spectrum obtained at 450 ns shows four broadband emission peaks that are centered at 11, 13.5,15.2 and 17.2 nm and these peaks are identified as transitions in $Xe^{11+}$, $Xe^{10+}$, $Xe^{9+}$ and $Xe^{8+}$ ions [11,12]. Besides form these broadband peaks, the lines from oxygen impurities at 15.2 and 17.2 nm are also appeared. These lines of $O^{4+}$ ionization state are attributed to the emission of impurity from the wall of capillary. In the image recorded during 700 ns, the height of the broadband peaks suppresses and the emission from impurities lines increase significantly as shown in figure 6 (b). The spectra recorded in later time are dominated by the impurities lines and these emissions do not contribute to the usable EUV output power for lithography.

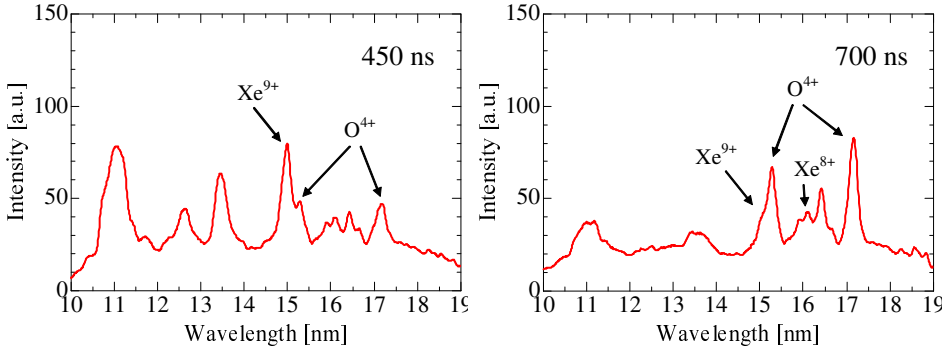


(a) (b)

**Figure 6.** Time resolved EUV spectra of the radiation emitted from Xe capillary discharge

The EUV spectra were also recorded using the transmission grating spectrograph. Figure 7 shows the spectra of transmission grating spectrometer for different Xe gas supply pressures (3 to 6 Torr). Transmission grating spectra also shows broad band peaks at 11, 13.5, 14.5 and 17.5 nm. From the spectra it is noticed that the intensity of each peak decreases with the increase of supply gas pressure. But further increase in the supply gas pressure beyond 6 Torr, only 14.5 nm peak seems to be prominent in comparison to the other peaks.

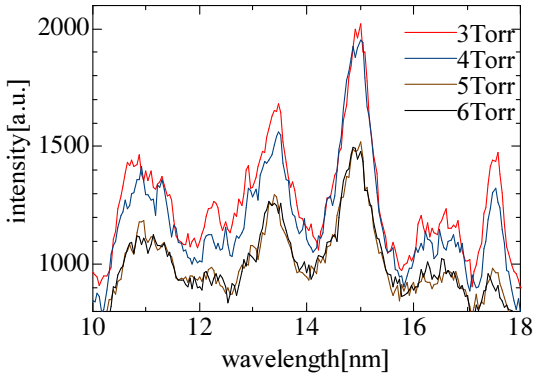


**Figure 7.** EUV spectra obtained from capillary discharge using transmission grating spectrometer

EUV photon yield in the range of 6 to 15 nm from the gas jet Z-pinch source was examined by employing the EUV photodiode integrated with Zr filter. The photodiode signals (with and without gas curtain) together with the current pulse are shown in figure 8. The EUV photons in both the cases appear after 70 ns of initiation of discharge current and reach a maximum nearly just before the maximum of current pulse. The EUV intensity peak as well as EUV photon flux improves around 30 % because of the presence of gas curtain. The duration of EUV emission occurs roughly 110 ns in absence of the gas curtain whereas it prolongs for another few tens of nanoseconds in presence of the gas curtain. The rise time of EUV signal is shorter than the fall time, which may be indicative of faster pinching of plasma and slower expansion of disrupted plasma. A second peak in EUV signal is always

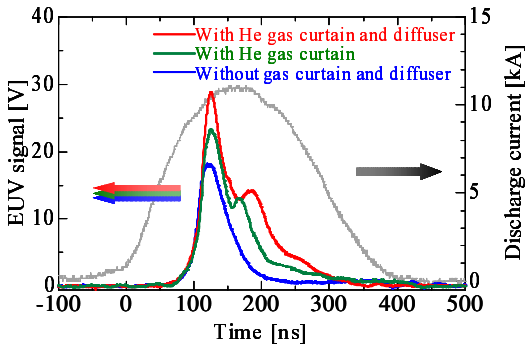


**Figure 8.** Traces of EUV photodiode and current signals

appeared in the presence of gas curtain only at higher Xe gas pressure (≥ 20 Torr). The appearance of second peak suggests another minor pinching of the expanding Xe plasma that occurs due to the confinement caused by the gas curtain. While employing an additional pumping system to diffuser the maximum photon flux is obtained which is more than twice of photon signal obtained without gas curtain. The in-band energy measurement was done with the help of EUV mini calorimeter at 10 Torr Xe supply pressure and 4 mm electrode separation. The EUV output in 2 % bandwidth at 13.5 nm is estimated to be 0.78 mJ/sr/pulse, which is much lower value than as observed in capillary discharge

head. In addition, the calorimeter was utilized to examine angular variation of in-band radiation and it is found to be exceptionally isotropic in available observable angle.

Time integrated EUV pinhole images were recorded at radial position with a time integrated EUV pinhole camera for various Xe gas pressures (10 to 30 Torr) and electrode separations (4 to 16 mm). The influence of both the experimental parameters on EUV emission is distinctly observed. Figure 8 shows some of the EUV images recorded at different Xe gas pressure for 12 mm electrode separation. It is observed that maximum EUV intensity is obtained at 20 Torr gas pressure which is roughly five times more than the intensity obtained at lower (10 Torr) and higher (30 Torr) gas pressures. Moreover, EUV intensity is improved by one order with simply increasing the electrode separation from 4 mm to 12 mm. The shot to shot fluctuation in EUV intensity measurement is approximately 4 %. A reasonably strong EUV intensity is obtained in between pressure range 18 to 25 Torr for electrode separation greater than 6 mm and the optimum condition for EUV intensity is 12 mm electrode separation and 20±2 Torr supply gas pressure. The dimension of EUV emitting zone was estimated at the optimum condition (12 mm electrode separation and 20 Torr supply pressure) and the FWHM diameter and length are found to be 0.16 and 0.92 mm, respectively. However, the dimension of EUV emitting zone increases by many folds while EUV intensity reduces significantly at a higher Xe supply pressure. The influence of gas flow rate of He gas curtain on EUV intensity and dimension is also studied. Nearly 25 to 50 % increase in EUV intensity is marked in 20 to 25 Torr Xe gas pressure because of the presence of gas curtain. But He flow rate has no major role on controlling maximum EUV intensity irrespective of Xe supply pressure. The influence of gas curtain on EUV emitting zone has observed only at higher Xe gas pressure (> 20 Torr) and the gas flow rate of gas curtain has very little effect on size of EUV emitting zone.

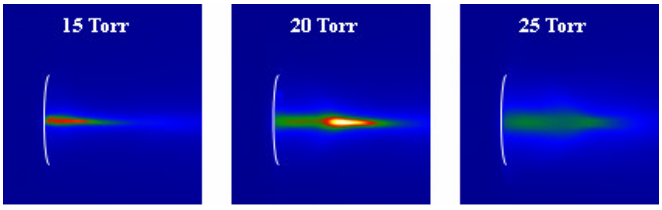


**Figure 8.** EUV pinhole images of gas jet Z-pinch plasma

## 4. Conclusions

To conclude, EUV diagnostics such as photon detector, mini calorimeter, pinhole camera and grazing incidence and transmission grating spectrographs were developed and employed to characterize EUV emission from pulsed plasma systems. These diagnostics tools have helped to asses the performance of capillary discharge and gas jet Z-pinch sources in terms of different technological aspects of EUV lithography source.

## Acknowledgments

This work is partly supported by New Energy and Industrial Technology Development Organization (NEDO) and by Grant-in-Aid for Scientific Research, the Ministry of Education, Culture, Sports, Science and Technology (MEXT). Authors are grateful to Dr. A. Okino, Dr. M. Watanabe, Dr.I. Song and other members of Hotta and Okino laboratory for their support and contribution to this work. SRM gratefully acknowledges the financial support of JSPS to pursue work at Tokyo Institute of Technology.

## References

[1] Grewing M, Kramer G, Schulz-Lupertz E, Wulf-Mathies C, Bowyer S and Kimble R 1981 *Space Science Reviews* **30** 575
[2] Hinnov E and Mattioli M. 1978 *Phys. Lett. A* **66** 109

[3] Radtke R, Biedermann C, Schwob J L, Mandelbaum P and Doron R 2001 *Phys. Rev. A* **64** 012720
[4] Ralchenko Yu, Draganic I N, Tan J N, Gillaspy J D, Pomeroy J M, Reader J, Feldman U and Holland G E 2008 *J. Phys. B: At. Mol. Opt. Phys.* **41** 021003
[5] Feldman U, Seely J F, Landi E and Ralchenko Yu 2008 *Nucl. Fusion* **48** 045004
[6] Rocca J J 1999 *Rev. Sci. Instrum.* **70** 3799
[7] Klosner M A and Silfvast W T 2000 *J. Opt. Soc. Am. B* **17** 1279
[8] Aota T and Tomie T 2005 *Phys. Rev. Lett.* **94** 015004
[9] Stamm U 2004 *J. Phys. D: Appl. Phys.* **37** 3244
[10] Bowering N, Martins M, Partlo W N and Fomenkov I V 2004 *J. Appl. Phys.* **95** 16
[11] Mohanty S R, Robert E, Dussart R, Viladrosa R, Pouvesle J M, Fleurier C and Cachoncinlle C 2003 *Microelectron. Eng*. **65** 47
[12] Song I, Iwata K, Honma Y, Mohanty S R**,** Watanabe M, Kawamura T, Okino A, Yasuoka K, Horioka K and Hotta E 2005 *Jpn J. of Appl. Phys.* **44** 8640
[13] Song I, Iwata K, Honma Y, Mohanty S R**,** Watanabe M, Kawamura T, Okino A, Yasuoka K, Horioka K and Hotta E 2006 *Plasma Sources Sci. Technol.* **15** 322
[14] Song I, Kobayashi Y, Sakamoto T, Mohanty S R**,** Watanabe M, Kawamura T, Okino A, Yasuoka K, Horioka K and Hotta E 2006 *Microelectron. Eng.* **83** 710
[15] Mohanty S R, Sakamoto T, Kobayashi Y, Izuka N, Kishi N, Song I, Watanabe M, Kawamura T, Okino A, Hoioka K and Hotta E 2006 *Appl. Phys. Lett.* **89**, 041502